American Journal of Engineering Research (AJER) 2018
American Journal of Engineering Research (AJER)
e-ISSN: 2320-0847 p-ISSN : 2320-0936
Volume-7, Issue-3, pp-317-330
www.ajer.org
Research Paper Open Access

Frustum Cone Piston Crown Equipped Compression Ignition Engine Performance Characteristics

Olumide A. Towoju[1], Ademola A. Dare[2]
[1](Department of Mechanical Engineering, Faculty of Engineering/ Adeleke University, Nigeria)
[2](Department of Mechanical Engineering, Faculty of Technology/ University of Ibadan, Nigeria)
Corresponding Author: Olumide A. Towoju

ABSTRACT: *Heavy duty applications have continued to rely on compression ignition engines because of its better efficiency, fuel economy, and reliability. However, the need for increased efficiency and reduction of toxic emission has continued to be a major source of concern. These challenges are being addressed with the redesigning of the combustion chamber. This study was therefore designed to determine the performance characteristics of a frustum cone-shaped piston crown equipped compression ignition engine.*
Numerical Model was developed from the mass balance, momentum, energy, and k-ε turbulent equations and solved with the finite element technique. The model was applied to a standard Yoshita 165F compression ignition engine to determine its performance characteristics. It was later applied to Yoshita 165F equipped with frustum cone-shaped piston crowns having cone-base angles of 25°, 30°, 35°, 40°, and 45° respectively to determine the best cone-base angle. Experiments were then carried out to determine the performance characteristics of the standard and best cone-base angle piston crown equipped Yoshita 165F using a TQ TD115 MKH absorption dynamometer. Data were statistically analysed using ANOVA at $\alpha_{0.05}$.
The frustum cone-shaped piston crown with a cone-base angle of 40° equipped engine gave an overall better performance and was used in the experiment. The results demonstrated that the performance and emission characteristics of a compression ignition engine can be improved with the use of frustum cone-shaped piston crowns. The estimates of the numerical model and experimental results were not statistically different.

KEYWORDS - *Compression ignition engine, Cone base-angle, Piston crown*

Date of Submission: 15-03-2018 Date of acceptance: 30-03-2018

I. INTRODUCTION

The significance of the compression ignition engine to the energy generation and transportation industries cannot be overemphasised. It has continued to play significant roles in the two sectors. In comparison with spark-ignition engines, compression ignition engines perform better in terms of thermal efficiency, brake power, and brake specific fuel consumption, however, its emission of toxic substance has continued to be a major source of concern coupled with the need for improvement of its thermal efficiency.

Several methods have been devised by researchers to reduce the emission of toxic substances and improve the performance of compression ignition engines, a few of the methods are; multiple injections in cold start, exhaust gas recirculation (EGR), combustion chamber geometry, [1] and dual fuel usage. Multiple fuel injections have an effect on the pressure variation inside the combustion chamber which ultimately determines its brake power. Exhaust gas recirculation has been proven by many scholars to have a positive impact on emission and fuel consumption of compression ignition engines; it involves the recycling of the exhaust gases such that it mixes with the fresh charge of air inside the combustion chamber and subsequently takes part again in the combustion process.

In order to reduce the dependency on the depleting reserves of crude oil used in the production of automotive gas oil (AGO) for fuelling compression ignition engines (Diesel engines) and also to ensure lower level of emission, many scholars are conducting research to study the impact of using biodiesels in blends with AGO on the performance of compression ignition engines.

The in-cylinder motion is dictated by the level of turbulence inside the combustion chamber and has domineering effects on the performance and emission characteristics of a compression ignition engine. The

extent of turbulence is determined among other factors by the combustion chamber design, and research has continued to concentrate on the impact of redesigning the combustion chamber of compression ignition engine on its performance.

The use of conical piston crown has been shown numerically to have a positive impact on the performance and emission characteristics of a compression ignition engine [2]. This work was carried out to experimentally validate numerical model results.

II. LITERATURE REVIEW

Homogenous charge compression ignition (HCCI) engine is a hybrid of the conventional compression ignition and the spark ignition engines. It is one of the several interventions made by researchers to enhance the performance and emission characteristics of the internal combustion engine and allows the use of fuels other than diesel (AGO) and petrol (PMS), just as other fuels with properties similar to that of diesel are being utilized in compression ignition engines.

Nitrogen oxides (NOx) which is one of the most harmful gases emitted by the compression ignition engine and smoke can be reduced by increasing the premixed ratio of fuel in an HCCI engine [3], and by the reduction of the compression ratio of a direct ignition compression ignition engine utilizing a premixed charge [4].

The utilisation of dual fuels in HCCI modes has been found to be beneficial going by the reports of various studies undergone by different scholars. Carbon-monoxide (CO), unburnt hydrocarbon (HC), and NOx emission reduces with the use of dual fuel in HCCI [5], [6], [7]. Increased brake thermal efficiency, reduced smoke, and brake specific fuel consumption of comparatively high percentage differences over that of the conventional compression ignition engine was further reported by [5] and [7] while operating an HCCI engine on different dual fuels. The results of the studies carried out by [8] was in agreement with the findings of [5] and [7], except for an increase in HC emission with the operation of a compression ignition engine on liquefied petroleum gas and Pongamia biodiesel. The brake thermal efficiency and soot emission of compression ignition engine improve with the use of Palm oil methyl ester (POME) [9] and with 20% Jatropha, 20% ethanol, diesel blend. [10]

HCCI engines show huge prospects of better fuel economy; however, it is taken aback by the effect of rapid pressure rise which is akin to experiencing “knock” as is experienced in spark ignition engines, and the problem of combustion timing. [11].

The emission of NOx can also be reduced with the use of EGR, [12], [13] however, there exists a critical value beyond which the further reduction in NOx emission is accompanied by increased emission of other unwanted products especially CO and HC. [13]

A whole lot of improvement in the performance characteristics of a compression ignition engine can be achieved with the optimisation of the combustion chamber design achieved by the modification of the piston crown. The shape of the combustion chamber was found to have significant effects on combustion and emission behaviour, [14] concluded that the depth of the chamber is an effective parameter on the formation of soot and NOx.

The use of selective catalysts has been employed for the reduction of emission from compression ignition engines fuelled with biodiesels, however, this does not have any impact on the engine performance because the use of a catalyst is an after-treatment process. [15]

Toroidal shaped combustion chamber designs have been proven to perform better in terms of brake thermal efficiency, CO, HC and particulate matters emission, however, it leads to slight increase in NOx emission [16], [17], [18], and [19]. Other combustion chamber designs such as re-entrant, trapezoidal, spherical and hemispherical also showed to have pulled an impact on the compression ignition engine performance. The trapezoidal and re-entrant combustion chamber results into an improvement in overall efficiency and lesser NOx emission, [18], [20]

In-cylinder fluid motion determined by air swirl governs the fuel-air mixing and burning rates in compression ignition engines which is a major contributing factor to its performance. Cutting of grooves on the piston crown generates air swirl. The smoke density, NOx, HC and CO emissions, brake thermal efficiency, brake specific fuel consumption showed an improvement using grooved pistons. [21], [22]

The utilization of the adiabatic concept has also been given a thought by researchers. This entails the use of thermal barrier coated engines which involves the coating of one or more of the parts and components of the combustion chamber. Ceramic coatings have been found to have positive effects on the performance of internal combustion engines just as was with the use of Yttria-stabilized Zirconia coatings. [23]

III. METHODOLOGY

3.1. Numerical Approach

The modelled engine is tailored towards the Yoshita 165F engine and fitted with frustum cone-shaped piston crowns having cone base angles of 25°, 30°, 35°, 40° and 45° while maintaining a uniform compression ratio of 20.5:1. COMSOL Multiphysics 5.0 was used to model the engine in 2-D axisymmetric coordinates.
The modelled engine parameters are as depicted in TABLE 1 below;

Table 1: Engine Parameters

Parameters	Specification
Engine Type (Brand)	YOSHITA 165F
Initial Temperature (K)	313
Initial Pressure (N/m^2)	1e5
Rated Speed 'N' (RPM)	2600
Rated Power 'P' (kW)	2.67
Compression Ratio 'CR'	20.5:1
Cylinder bore 'D' (m)	0.070
Stroke 'S' (m)	0.070
Crank arm length 'La' (m)	0.035
Connecting rod length 'Lc' (m)	0.130

The combustion of fuel in a compression ignition engine is governed by the mass balance, momentum and the energy equation. These equations were used to model the thermo-fluid activity undergone in the combustion chamber, and are as spelled out below:

$$\rho\frac{\partial u}{\partial t} + \rho\,u.\nabla u = -\nabla.\rho + \nabla.\left[\mu\,(\nabla u + (\nabla u)^T) - \frac{2}{3}\,\mu\nabla(\nabla.u)\right] + B \quad (1)$$

$$\rho c_p\frac{\partial T}{\partial t} + \rho c_p\, u.\nabla T = \nabla.(k\nabla T) + Q \quad (2)$$

The Reynolds Averaged Navier-Stokes (RANS) employing the k-ε turbulent model was employed to simplify the problem and ensure its convergence:

$$\rho\frac{\partial u}{\partial t} + \rho\,u.\nabla u = \nabla.\left[-\rho 2I + (\mu+\mu_T)\,(\nabla u + (\nabla u)^T) - \frac{2}{3}\,(\mu+\mu_T)\nabla(\nabla.u)I - \frac{2}{3}\rho kI\right] + B \quad (3)$$

The 'k' equation is:

$$\rho\frac{\partial k}{\partial t} + \rho(u.\nabla)k = \nabla.\left[(\mu + \frac{\mu_T}{\sigma_k})\nabla k\right] + p_k - p_\varepsilon \quad (4)$$

And the 'ε' equation is:

$$\rho\frac{\partial \varepsilon}{\partial t} + \rho(u.\nabla)\varepsilon = \nabla.\left[(\mu + \frac{\mu_T}{\sigma_\varepsilon})\nabla\varepsilon\right] + C_{\varepsilon 1}\frac{\varepsilon}{k}P_k - C_{\varepsilon 2}\rho\frac{\varepsilon^2}{k} \quad (5)$$

Where $\mu_T = \rho C_\mu \frac{k^2}{\varepsilon}$ and

$$P_k = \mu_T\left[\nabla u : (\nabla u + (\nabla u)^T) - \frac{2}{3}(\nabla.u)^2\right] - \frac{2}{3}\rho k\nabla.u$$

Estimates for engine power (P), thermal efficiency (η_{Th}), brake specific fuel consumption (BSFC), and torque (T_q) is made based on the predictions of the numerical model and derived using the following equations:

$$P = \frac{P_m LAN}{n_c} \quad (6)$$

Where $P_m = \frac{W_{net}}{V_s}$,

$$\eta_{Th} = \frac{W_{net}}{Q_{in}} \quad (7)$$

$$BSFC = \frac{\rho_{atm}}{(A/F)P_m} = \frac{\rho_f q}{P} \quad (8)$$

$$T_q = \frac{60P}{2\pi N} \quad (9)$$

W_{net} is the network output from the engine
Q_{in} is the heat energy generated by the combustion of the fuel-air mixture
V_s is the displacement volume
A is the area of the cylinder (πr^2)
N is the number of revolutions per minute
n_c is the number of cycles required to make a complete revolution
ρ_{atm} is the atmospheric air density
(A/F) is the air-fuel ratio.

3.2. Experimental Approach

To validate the results gotten from the numerical approach, experiments were conducted on a horizontal single cylinder four-stroke air-cooled compression ignition engine.

A control experiment was carried out on the test engine using AGO, and experiment was also conducted on the best cone base angle modified piston crown fitted test engine as obtained from the estimates of the numerical model using AGO as the test fuel.

Physicochemical tests were first conducted on the test fuel to determine its physical and chemical properties using standard tests methods. The properties tested for are; density, specific gravity, kinematic viscosity, cloud point temperature, pour point temperature, flash point temperature, fire point temperature, carbon content, PH value, calorific value, ash content, cetane number, and sulphur content.

The figure below shows the schematic representation of the experimental set-up.

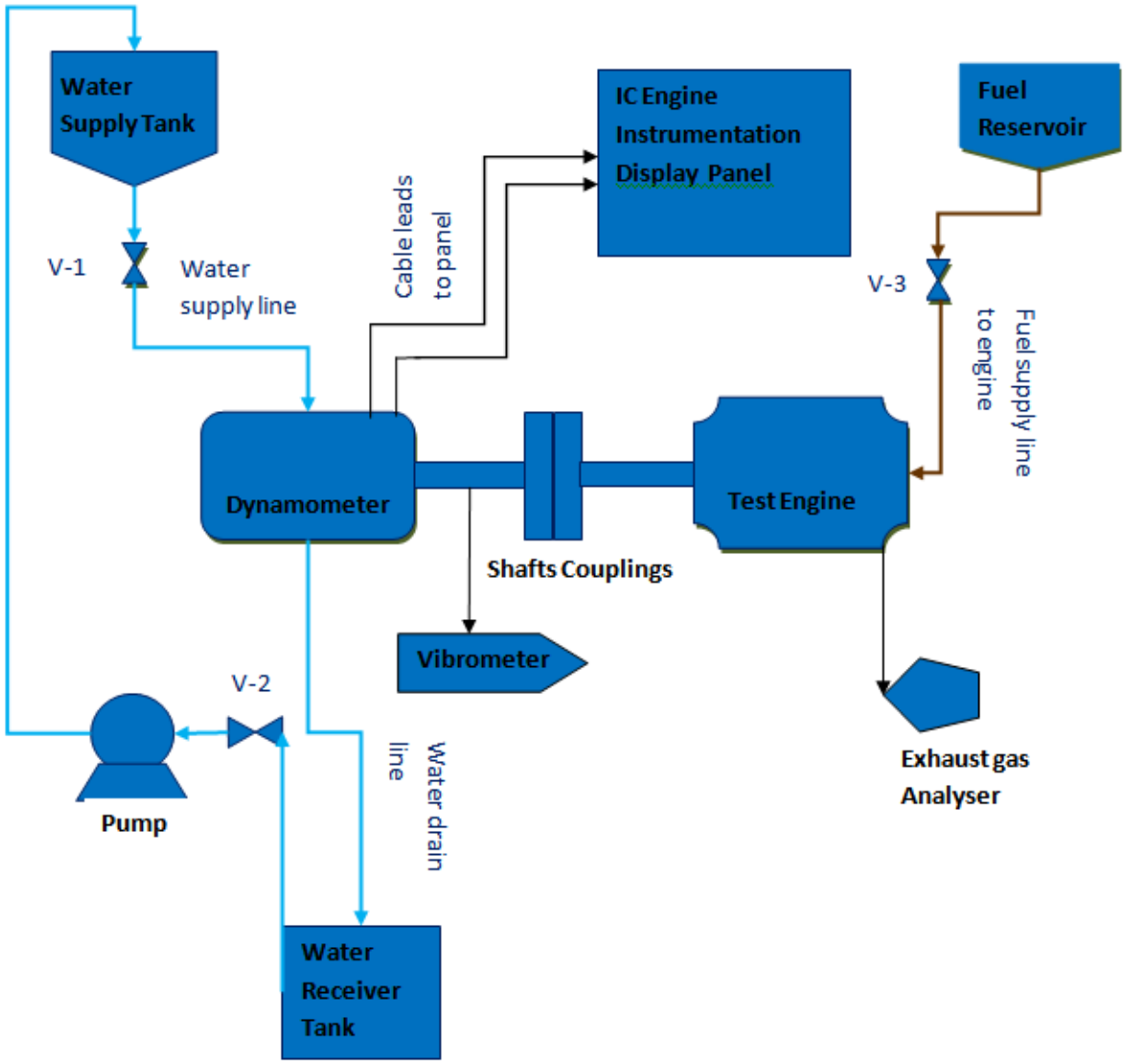

Fig. 1 Schematics of Experimental set-up

The specification of the dynamometer is stated in TABLE 2 below.

Table 2: Dynamometer Specification

Parameters	**Value**
Dynamometer Type	TQ TD115 MKH Absorption Dynamometer
Power Range (kW)	2.5 – 7.5
Torque (Nm)	15 (maximum)
Speed (RPM)	6000 (maximum)

The assembled experimental rig is shown in Figure 2 below;

Fig. 2 Experimental test rig

Using the results gotten from the simulation studies, the test engine piston was modified towards getting optimal improvement in the engine performance.

The angle of tapering chosen was 40° and a tapered height of 0.005m for frustum cone-shaped piston crown geometry.

The volume of the removed material was calculated using the relation:

$$V_r = \frac{\pi d^2 Lo}{4} - \left(\frac{\pi d^2 L}{12} - \frac{\pi}{12}(d - do)^2(L - Lo)\right) \quad (10)$$

Where Lo = 0.005m, d = 0.07m, and θ = 40°

$$L = \frac{d}{2tan\theta} \quad (11)$$

$$L = \frac{0.07}{2*tan\,40^\circ} = 0.0417\text{m}$$

$$do = 2ro = 2Lotan\theta = 2*0.005\ *tan40^\circ = 0.0084\text{m}$$

$$V_r = \frac{\pi*0.07^2*0.005}{4} - \left(\frac{\pi*0.07^2*0.0417}{12} - \frac{\pi}{12}(0.07 - 0.0084)^2(0.0417 - 0.005)\right)$$

$$= 2.2073*10^{-6}\ \text{m}^3$$

The fuel consumption rate by the engine is obtained from the relation:

$$Q = \frac{V_{fuel}}{t} \quad (12)$$

While the mechanical efficiency is calculated using the relation:

$$\eta_M = \frac{Brake\ \ power}{Indicated\ \ power} \quad (13)$$

To ensure a uniform compression ratio, the clearance volume and swept volume of the engine cylinder were kept constant even after the modification.

Figure 3 is a representation of the unmodified and the modified piston crowns, and figure 4 is a sketch of the frustum cone-shaped crown

Fig. 3 Piston crown modification

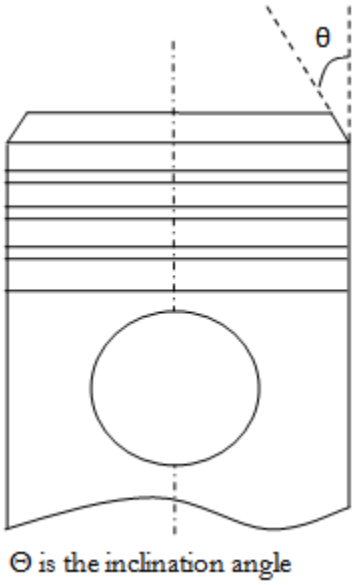

Fig. 4 Frustum cone-shaped piston crown

IV. RESULTS AND DISCUSSION

4.1. Numerical Model Estimations

The cut-plane sections of the engine in the vertical direction indicating its velocity distributions as generated in the numerical model are depicted in figure 5 below.

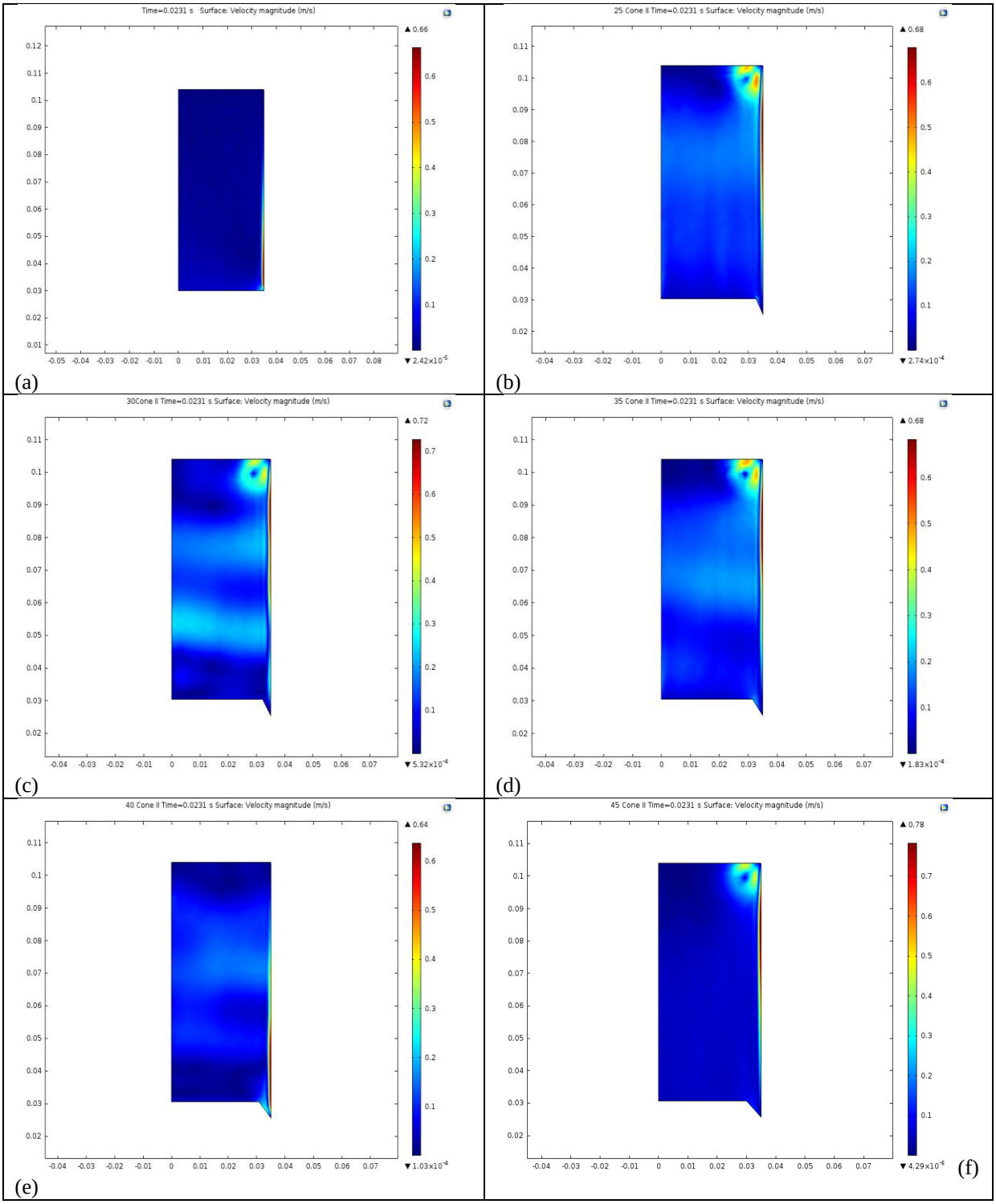

Fig. 5 (a) Unmodified piston crown, (b) 25°, (c) 30°, (d) 35°, (e) 40° and (f) 45° frustum cone-shaped piston crown velocity distribution at "t" = 0.0231s

The occurrence of active zones (portions with higher velocities) in the engine cylinder was affected by the piston crown geometry. The velocity of the charge inside the engine cylinder was observed to be least for the frustum cone-shaped piston crown with an inclination angle of 40° (Figure 5(e)) giving an indication that bulk of its kinetic energy has been converted into pressure energy used for doing useful work than for the other piston crown geometries.

4.1.1 Thermal Efficiency of the Simulated Engine

The thermal efficiency of the engine when fitted with the unmodified and modified pistons crown with the stated inclination angles was calculated using (7): the values are shown in TABLE 3, and the plot follows in Figure 6.

Table 3: Thermal Efficiency of Modelled Engine

Inclination Angle (°)	η_{Th} **(%)**
0	32.200
25	32.255
30	32.255
35	32.258
40	32.261
45	32.250

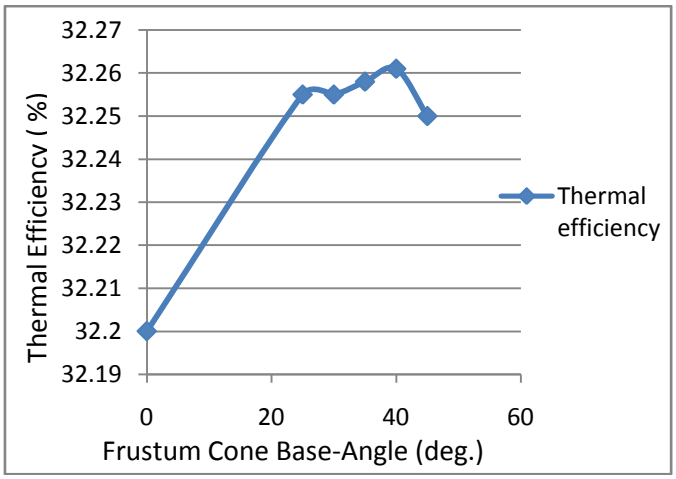

Fig. 6 Thermal efficiency plot

The thermal efficiency of the engine is a maximum when it is equipped with the frustum cone-shaped piston crown with an inclination angle of 40° as depicted in Figure 6 above, and for all the used inclination angles, the thermal efficiencies was greater than that of the unmodified piston crown fitted engine. This can be attributed to better fuel combustion as result of refined in-cylinder motion resulting from the combustion chamber redesign.

4.1.2. Brake Power from Engine Simulations

The power generated by the engine when fitted with the unmodified piston and the modified piston crown was computed using the relation in (6).

The estimated generated power for the standard piston and frustum cone-shaped piston crown fitted engine is given in TABLE 4 and its plot follows in Figure 7;

Table 4: Generated Power of Modelled Engine

Inclination Angle (°)	Power (kW)
0	2.3765
25	2.3786
30	2.3786
35	2.3789
40	2.3790
45	2.3782

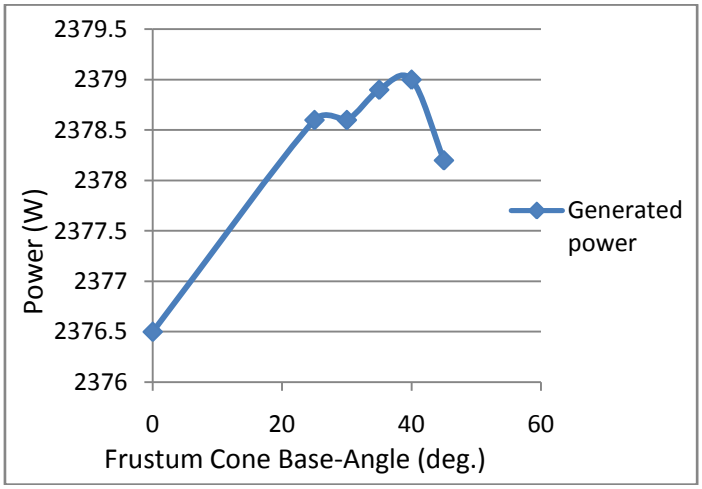

Fig. 7 Engine generated power plots

As depicted in Figure 7, the power generated by the engine when fitted with the frustum cone-shaped piston crown is higher at all inclination angles than for the unmodified piston crown with the maximum value recorded at an angle of inclination of 40°. The piston crown modification results in the redesign of the combustion chamber in such a manner to increase fluid flow turbulence thereby resulting in improved in-cylinder motion and improved power in comparison to the cylindrical piston.

4.1.3. Engine Torque from Engine Simulations

The engine torque for each of the piston crown geometry was calculated using (9).
The estimated engine torque for the standard piston and frustum cone-shaped piston crown fitted engine is given in TABLE 5 and its plot follows in Figure 8;

Table 5: Torque of the Modelled Engine

Inclination Angle (°)	Torque (N/m)
0	8.728
25	8.736
30	8.736
35	8.737
40	8.738
45	8.735

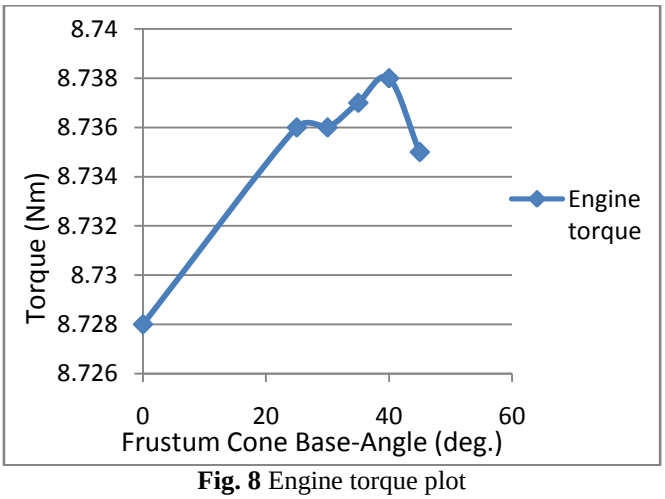

Fig. 8 Engine torque plot

The engine torque was peaked when it was equipped with the frustum cone-shaped piston crown having an inclination angle of 40°. The engine torque was observed to increase with the inclination angle up till 40°, and after which at 45° it showed a decrease as it was observed for the thermal efficiency and generated power. This is an indication that the in-cylinder fluid motion witnessed an improvement as the piston crown was

modified from the cylindrical type to the frustum cone shape and that there exist a critical inclination angle beyond which the in-cylinder motion ceases to be favoured with increases in cone angle.

4.1.4. Brake Specific Fuel Consumption of the Simulated Engine

The specific fuel consumption was calculated using (8);

$BSFC = \frac{\rho_{atm}}{(A/F)P_m} = \frac{\dot{m}_f}{P} = \frac{\rho_f q}{P}$

Using $BSFC = \frac{\rho_{atm}}{(A/F)P_m}$,

ρ_{atm} = 1.1886 kg/m^3

$((A/F)_{stoc} = \frac{m_{air}}{m_{fuel\ stoc}} = \frac{4.76*11*m_{air}}{1*m_{fuel}})$

$(\psi = \frac{(A/F)_{stoc}}{(A/F)})$

m_{air} = 28.96 kg/Kmol, m_{fuel} = 100 kg/Kmol (C_7H_{16}), ψ = 0.5

$(A/F) = \frac{(A/F)_{stoc}}{\psi}$

$= \frac{4.76*11*m_{air}}{\psi*1*m_{fuel}}$

$= 0.5 * \frac{4.76*11*28.96}{100} = 30.33$

The estimated specific fuel consumption for the standard piston and frustum cone-shaped piston crown fitted engine is given in TABLE 6 and its plot follows in Figure 9;

Table 6: Specific Fuel Consumption of Modelled Engine

Inclination Angle (°)	BSFC (kg/kWh)
0	0.3466
25	0.3463
30	0.3463
35	0.3463
40	0.3462
45	0.3464

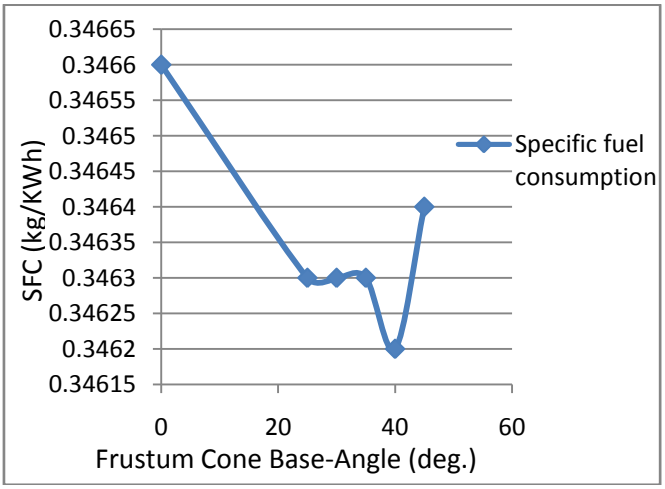

Fig. 9 Engine brake specific fuel consumption

The specific fuel plots as depicted above can be observed to be the reciprocal of the power plots in Figure 7; this is because the specific fuel consumption is a measure of the generated power per unit mass of fuel, and is inversely proportional to the value of the generated power. The frustum cone-shaped piston crown having an inclination angle of 40° has the least value of specific fuel consumption, giving an indication of its better performance.

4.1.5. Carbon monoxide (CO) Emissions of the Simulated Engine

Carbon-monoxide emissions plot as estimated from the simulation of the engine when equipped with the unmodified piston crown and the frustum cone-shaped piston crown for the stated inclination angles is shown in Figure 10 below.

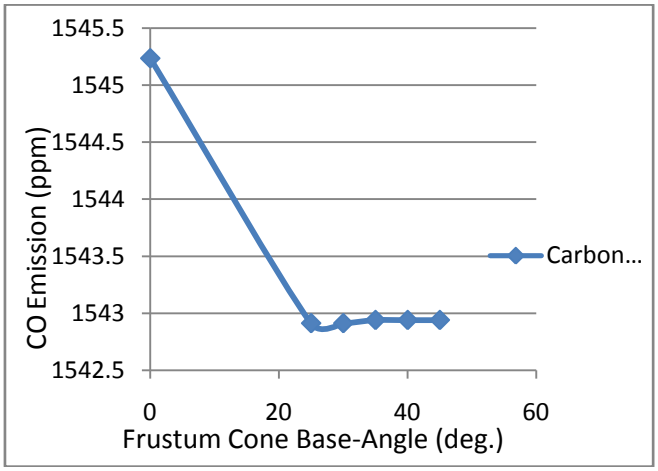

Fig. 10 Engine's Carbon monoxide (CO) emissions

For all the cases of the frustum cone-shaped piston crown fitted engine, the carbon monoxide emission level was observed to be lower than that of the unmodified piston crown fitted engine. The modifications of the piston crown thus have an effect on the engine's emission of carbon monoxide.

4.2. Results of Experiment

The test fuel (AGO) chemo-physical properties are tabulated in TABLE 7 below.

Table 7: Chemo-Physical Properties of the Test Fuel

Properties	**AGO**
Density (g/ml)	0.84
Specific gravity	0.84
Kinematic viscosity at 30℃ mm^2/s	3.7
Pour Point ℃	-35
Flash Point ℃	+114
Fire Point ℃	+132
Cloud Point ℃	-28
Carbon Content %	97.20
PH Value	8.10
Sulphur content (ppm)	4.28
Ash content	0.05
Cetane Number	39.6
Calorific Value (MJ/kg)	36

TABLE 8 and TABLE 9 below shows the output from the experiment carried out on the standard piston equipped engine and the frustum cone-shaped piston crown with inclination of 40° equipped engine.

Table 8: Unmodified Piston Crown Output

Parameter	**Value**
Speed (RPM)	1900
Exhaust Temperature (℃)	410
Torque (Nm)	9
Average Time for 2ml (s)	4.64
Vibration (m/s^2)	19.4
CO (ppm)	1598
O_2 (%)	19.3

Table 9: Modified Frustum Cone-Shaped Piston Crown Output

Parameter	**Value**
Speed (RPM)	1950
Exhaust Temperature (℃)	360
Torque (Nm)	8.8
Average Time for 2ml (s)	4.24
Vibration (m/s^2)	25.8
CO (ppm)	1463
O_2 (%)	19.1

Using (12) and the data depicted in TABLES 8 and 9, the flow rate of the fuel into the engine is shown in TABLE 10 below.

Table 10: Flow Rate Computations

Piston Crown Type	**q ($1*10^{-7}$(m^3/s))**
Unmodified Piston Crown fitted Engine	4.310
Modified Piston Crown fitted Engine	4.717

4.2.1. Engine Vibration

The engines vibration level is expected to always be below a certain designed threshold to ensure its durability, and is a rich source of information regarding physical conditions monitoring (Alhouli, *et al*., 2015) (20). The engines vibration level when fitted with the unmodified piston crown was observed to be lower when compared to it being fitted with the modified piston crown. The vibration level of the engine increased by 33% with the use of the frustum cone-shaped piston crown over that of the unmodified piston. This should be expected as the original design of the engine was for the unmodified piston and the modification would have in one way or the other alters the engine balance due to changes in its pressure.

4.2.2. Brake Power

The brake engine power is calculated using (9). The brake power generated by the test engine when fitted with the unmodified and the modified piston crown with an inclination angle of 40° is shown in TABLE 11.

Table 11: Brake Power

Piston Crown Type	**Brake Power (W)**
Unmodified Piston Crown fitted Engine	1790.71
Modified Piston Crown fitted Engine	1796.99

The combustion chamber redesign as a result of using the frustum cone-shaped piston crown with an inclination angle of 40° must have favoured a better in-cylinder fluid motion occasioned by improved air turbulence, because nothing more could have been responsible for the increased brake power over that with the unmodified piston crown. A percentage increase of 0.36% was recorded after the modification of the piston crown to a frustum cone-shaped geometry with an inclination angle of 40°.

4.2.3. Mechanical efficiency of the Engine

The mechanical efficiency of the engine operated on AGO when fitted with the unmodified piston crown and the modified piston crown was calculated using (13).

The mechanical efficiencies of the test engine when fitted with the unmodified and the modified piston crown with an inclination angle of 40° is as tabulated in TABLE 12.

An improvement of 0.27% in mechanical efficiency was observed with the use of the modified piston over the unmodified one.

Table 12: Mechanical Efficiencies Computations

Piston Crown Type	**η_M (%)**
Unmodified Piston Crown fitted Engine	67.07
Modified Piston Crown fitted Engine	67.30

4.2.4. Brake Specific Fuel Consumption

The brake specific fuel consumption of the engine operated on AGO when fitted with the unmodified piston crown and with the modified piston crown was calculated using (8). TABLE 13 is the tabulation of the brake specific fuel consumption of the engine equipped with the standard piston crown and the frustum cone-shaped piston crown with an inclination angle of 40°. The brake specific fuel consumption of the engine increased with the use of the modified piston crown, despite it producing more power. Changes in the combustion chamber design without corresponding changes in nozzle design, valve timing, and injection pressure e.t.c. possibly could have led to this.

Table 13: Brake Specific Fuel Consumption

Piston Crown Type	**BSFC (kg/kWh)**
	ρ_f =840 kg/m^3
Unmodified Piston Crown fitted Engine	0.7278
Modified Piston Crown fitted Engine	0.7936

4.2.5. Thermal Efficiency of Engine

The thermal efficiency for the cases of the engine when fitted with the unmodified piston crown and with the modified piston crown and operated on AGO is calculated using (7).

The thermal efficiencies of the test engine when fitted with the unmodified and the modified piston crown with an inclination angle of 40° is shown in TABLE 14. The thermal efficiency of the experimental results was found to be lower than that estimated from the numerical model, and this can be attributed to the assumption of an insulated cylinder wall for the numerical simulation, whereas in the case of experiments, heat is actually lost through the cylinder walls of the engine.

Table 14: Thermal Efficiency

Piston Crown Type	η_{Th} **(%)**
Unmodified Piston Crown fitted Engine	13.74
Modified Piston Crown fitted Engine	12.60

4.2.6. Carbon monoxide Emission of Experimental Engine

As shown in TABLE 15, the Carbon monoxide emission values decreased with the use of the 40° frustum cone-shaped piston crown in comparison to that with the unmodified piston crown. This can be attributed to better mixing and near complete combustion arising from increased turbulence introduced by the piston modification.

Table 15: CO Emission

Piston Crown Type	**CO (ppm)**
Unmodified Piston Crown fitted Engine	1598
Modified Piston Crown fitted Engine	1463

4.3. Comparison of the Numerical Results with Experimental Data

The ANOVA at $\alpha_{0.05}$ of the engine torque, mean effective pressure, and CO emission from the numerical and experimental analyses are as shown in TABLE 16. The engine torque, mean effective pressure and carbon monoxide emission were observed not to be statistically different at $\alpha_{0.05}$.

Table 16: The ANOVA Results for the Performance Parameters of the Estimates of Numerical Model and Experimental Results

Performance Parameter	**Source of Variation**	**Sums of Squares**	**Degrees of Freedom**	**Mean Squares**	**Variance Ratios (F)**	**Probability value (F Critical)**
Torque (N/m)	Between samples	0.0306	1	0.0306	3.0524	18.51
	Within Samples	0.0200	2	0.0100	-	-
	Total	0.0506	3	-	-	-
Mean Effective Pressure (N/m^2)	Between samples	0.0063	1	0.0063	2.9302	18.51
	Within Samples	0.0043	2	0.0021	-	-
	Total	0.0106	3	-	-	-
CO (ppm)	Between samples	184.60	1	184.60	0.0405	18.51
	Within Samples	9115.14	2	4557.57	-	-
	Total	9299.74	3	-	-	-

V. CONCLUSION

- The estimates of the numerical model showed that the frustum cone-shaped piston crown with cone base angle of 40° equipped compression ignition engine performed best. This is in agreement with the earlier findings of the authors where they carried out numerical studies on a Kirloskar TV-1 engine. [2]
- The estimates of the numerical model and the results of the experiments were in agreement to an acceptable level statistically.
- The performance characteristics of a compression ignition engine can be optimised with the use of a frustum cone-shaped piston crown.

REFERENCES

[1] Lofti, A., & Ghassemi, H. (2017). A Review on the Different Geometries of Combustion Chamber in CI Engines on Performance, Ignition and Emission. *Journal of Atmospheric Pollution , 5* (2), 40-46.

[2] Towoju, O. A., & Dare, A. A. (2018). Impact of Conical Piston Crown Equipped Compression Ignition Engine on Performance. *European Journal of Engineering and Technology , 6* (1), 13-25.

[3] Himmatsinh, R. C., Syham, K. D., Preksha, K., & Vivek, G. T. (2015). A Technical Review of HCCI Combustion in Diesel engine. *IJIRST-International Journal for Innovative Research in Science & Technology , 1* (10), 28-31.

[4] Laguitton, O., Crua, C., Cowell, T., Heikal, M., & Gold, M. (2006). Effect of Compression ratio on Exhaust Emissions from a PCCI Diesel engine. *Proceedings of the 19th International Conference on Efficiency, Cost, Optimization, Simulation and Environmental Impact of Energy Systems* (pp. 2918-2924). Crete: Energy conversion and management.

[5] Banapurmath, R., Dodamani, B., Khanda, S., Hiremath, S., & Math, V. (2014). Performance, Emission Characteristics of Dual Fuel (DF) & Homogeneous Charge Compression Ignition (HCCI) Engines Operated on Compressed Natural Gas (CNG) – Uppage Oil Methylester (UOME). *Universal Journal of Renewable Energy , 2*, 32-44.

[6] Bhabani, P. P., Chandrakanta, N., & Basanta, K. N. (2013). Investigation on utilization of Biogas & Karanja Oil biodiesel in dual fuel mode in a Single Cylinder DI Diesel engine. *International Journal of Energy and Environment , 4* (2), 279-290.

[7] Ravi, M., Vijayakumar, K., Ashok, K. M., & Gunaseelan, T. (2015). Experimental Investigation on Emission and Performance Charecteristics of Single Cylinder Diesel Engine using Lime Treated Biogas. *International Journal of ChemTech Research , 7* (4), 1720-1728.

[8] Periyasamy, M., & Vadivel, N. (2015). Experimental Investigation On LPG-Biodiesel (Pongamia) Dual Fuelled Engine. *International Journal on Applications in Mechanical and Production Engineering , 1* (3), 3-7.

[9] Patil, S. (2013). Thermodynamic Modelling for Performance Analysis of Compression Ignition Engine Fuelled With Biodiesel and its Blends With Diesel. *International Journal of Recent Technology and Engineering (IJRTE) , 1* (6), 134-138.

[10] Gaurav, P., Ambarish, D., & Bijan, K. M. (2014). Numerical Investigation of the Performance and Emission Characteristics of a CI engine using Diesel and its blends with Ethanol and Jatropha Biodiesel. *International Journal of Current Engineering and Technology* (3), 5-9.

[11] Prasad, G. R., Goud, S. C., & Meheswar, D. (2012). Alternative Fuels for HCCI engine technology and recent developments. *International Journal of Advanced Research in Engineering and Applied Science , 1* (2), 1-19.

[12] Kumar, R. N., Sekhar, Y., & Adinarayana, S. (2013). Effects of Compression Ratio and EGR on Performance, Combustion and Emissions of Di Injection Diesel Engine. *International Journal of Applied Science and Engineering , 11* (1), 41-49.

[13] Sorathia, H. S., Rahhod, P. P., & Sorathiya, A. S. (2012). "Effects of Exhaust Gas Recirculation (EGR) on NOx Emission on C.I. Engine" - A Review Study. *International Journal of Advanced Engineering Research and Studies , 1* (3), 223-227.

[14] Jafarmadar, S., & Khanbabazadeh, M. (2008). A Computational Study of the Effects of Combustion Chamber Geometries on Combustion Process and Emission in a DI Diesel Engine. *Journal of Fuel and Combustion , 1* (1), 1-16.

[15] Thirumal, B. J., Gunasekaran, E. J., & Saravanan, C. G. (2013). Performance and Emission Analysis of Bio Diesel Fuelled Engine with Selective Catalyst Reduction (SCR). *International Journal of Engineering and Technology , 3* (2), 205-211.

[16] Jaichandar, S., & Annamalai, K. (2012). Effects of open combustion chamber geometries on the performance of pongamia biodiesel in a DI diesel engin. *Fuel , 98*, 272-279.

[17] Mamilla, V. R., Mallikarjun, M., & Rao, G. N. (2013). Effect of Combustion Chamber Design on a DI Diesel Engine Fuelled with Jatropha Methyl Esters Blends with Diesel. *International Conference On Design and Manufacturing, IConDM 2013* (pp. 479-490). India: Elsevier Ltd.

[18] Ranganatha, S. L., Chandrashekar, T., Banapurmath, N., & Nashipudi, P. (2014). Effect of Injection Timing, Combustion Chamber Shapes and Nozzle Geometry on the Diesel Engine Performance. *Universal Journal of Petroleum Sciences , 2*, 74-95.

[19] Nataraj, K., Banapurmath, N., Manavendra, G. Y., Vaibhav, K., & Satish, G. (2015). Effect of Combustion Chamber Shapes on the Performance of Mahua and Neem Biodiesel Operated Diesel Engines. *Petroleum & Environmental Biotechnology , 6* (4), 1-7.

[20] Indrodia, A., Chotai, N., & Ramani, B. (2014). Investigation of Different Combustion Chamber Geometry on Diesel Engine using CFD Modelling of In-cylinder Flow for Improving the Performance of Engine . *5th International & 26th All India Manufacturing Technology, Design and Research Conference (AIMTDR 2014)*, (pp. 489-1 - 489-6). Assam.

[21] Bharathi, V. V., & Prasanthi, G. (2013). The Influence of Air Swirl on Combustion and Emissions in a Diesel Engine. *International Journal of Researh in Mechanical Engineering and Technology , 3* (2), 14-16.

[22] Reddy, C. S., Reddy, C. E., & Reddy, K. H. (2012). Effect of Tangential Grooves on Piston Crown of D.I. Diesel Engine with Blends of Cotton Seed Oil Methyl Easter. *IJRRAS , 13* (1), 150-159.

[23] Krishna, V. S., Reddy, K. V., & Prasad, B. D. (2016). Evaluation of Performance and Emission Characteristics of CI Diesel Engine using Biodiesel with Adiabatic Concept. *International Journal of Innovative Research in Science, Engineering and Technology , 5* (7), 13873-13880.

Olumide A. Towoju "Frustum Cone Piston Crown Equipped Compression Ignition Engine Performance Characteristics." American Journal of Engineering Research (AJER), vol. 7, no. 3, 2018, pp.317-330.